REFERENCES AND NOTES

1. J. E. Sulston and H. R. Horvitz, *Dev. Biol.* **56**, 110 (1977).
2. R. J. Sommer and P. W. Sternberg, *Curr. Biol.* **6**, 52 (1996).
3. R. J. Sommer, *Development* **124**, 243 (1997); *Bioessays* **19**, 225 (1997).
4. We would argue that the fusion of nonvulval cells that is seen in *Caenorhabditis* is ancestral, as this cell fate is observed in species of many different families. In particular, *Strongyloides ratti*, a species of the order Strongylida that can be considered as an outgroup for both *Caenorhabditis* and *Pristionchus* [V. V. Malakhov, *Nematodes* (Smithsonian Institution Press, Washington, DC, 1994)] displays fusion of nonvulval epidermal cells (R. J. Sommer, unpublished observation).
5. B. B. Wang *et al.*, *Cell* **74**, 29 (1993); S. G. Clark, A. D. Chisholm, H. R. Horvitz, *ibid.*, p. 43; S. J. Salser, C. M. Loer, C. Kenyon, *Genes Dev.* **7**, 1714 (1993); T. R. Clandinin, W. S. Katz, P. W. Sternberg, *Dev. Biol.* **182**, 150 (1997).
6. *Ppa-lin-39* was cloned by PCR using degenerate primers in the homeodomain. The primers were 5′-CGTCAGMGTACTGCNTAYAC-3′ and 5′-CATGCKACKRTTYTGRAACCA-3′.
7. Mutagenesis screens were carried out as described (*2*).
8. Hermaphrodites of the fifth mutant, *sy319*, never form ventral protrusions or vulvae and thus, cannot be mated.
9. First genetic characterization of these mutants indicates that they belong to several genes. None of the mutants is linked to *Ppa-dpy-1* (C. Weise and R. J. Sommer, unpublished observation).
10. DNA was isolated from two independent batches of mutant animals, amplified by three independent PCR reactions, and sequenced in both directions. Although the mutant *sy319* cannot be tested genetically, the molecular analysis suggests that the mutant is an allele of *Ppa-lin-39*. The molecular lesion introduces a stop codon into the hexapeptide, removing the complete homeodomain. The strong vulvaless phenotype of *sy319* mutant animals is consistent with the more severe molecular truncation in comparison to the three other alleles (Figs. 3 and 4; Table 1). However, we cannot rule out that a second background mutation is involved in generating the strong vulvaless phenotype of *sy319* mutant animals.
11. D. M. Bird and D. L. Riddle, *J. Nematol.* **26**, 138 (1994).
12. The three alleles *tu2, tu29,* and *sy374* were all marked with the linked recessive visible mutation *Ppa-dpy-1*. Crossed progeny from a mating of such marked vulvaless homozygous hermaphrodites with wild-type males are wild type for the visible marker (being *Ppa-dpy-1/+*) and wild type for the vulva phenotype scored under Nomarski optics (10/10 for each allele). Such heterozygous hermaphrodites segregated one-quarter vulvaless animals, all of which are also homozygous mutant for the visible marker. Segregants that are wild type for the visible marker are also wild type for the vulva phenotype scored under Nomarski optics (25/25 for each allele).
13. J. Yuan, *J. Cell. Biochem.* **60**, 4 (1996).
14. K.-Z. Lee and R. J. Sommer, unpublished observation.
15. Single-letter abbreviations for the amino acid residues are as follows: A, Ala; C, Cys; D, Asp; E, Glu; F, Phe; G, Gly; H, His; I, Ile; K, Lys; L, Leu; M, Met; N, Asn; P, Pro; Q, Gln; R, Arg; S, Ser; T, Thr; V, Val; W, Trp; and Y, Tyr.

16. We thank C. Kenyon and C. Hunter for a *Caenorhabditis lin-39* cDNA clone used in the original hybridization experiments; D. Gilmour, S. Jesuthasan, T. Nicolson, and S. Roth for critical reading of the manuscript; and members of the laboratory for discussion. R.J.S. is a Young investigator with the Max-Planck Society.

11 June 1997; accepted 3 September 1997

Phosphorylation of Sic1p by G_1 Cdk Required for Its Degradation and Entry into S Phase

R. Verma, R. S. Annan, M. J. Huddleston, S. A. Carr, G. Reynard, R. J. Deshaies

G_1 cyclin-dependent kinase (Cdk)–triggered degradation of the S-phase Cdk inhibitor Sic1p has been implicated in the transition from G_1 to S phase in the cell cycle of budding yeast. A multidimensional electrospray mass spectrometry technique was used to map G_1 Cdk phosphorylation sites in Sic1p both in vitro and in vivo. A Sic1p mutant lacking three Cdk phosphorylation sites did not serve as a substrate for Cdc34p-dependent ubiquitination in vitro, was stable in vivo, and blocked DNA replication. Moreover, purified phosphoSic1p was ubiquitinated in cyclin-depleted G_1 extract, indicating that a primary function of G_1 cyclins is to tag Sic1p for destruction. These data suggest a molecular model of how phosphorylation and proteolysis cooperate to bring about the G_1/S transition in budding yeast.

Exit from the G_1 phase and the initiation of DNA synthesis in the cell cycle of budding yeast require the activities of *CDC34*, *CDC4*, *CDC53*, *SKP1*, one member of a set of G_1 cyclin genes (*CLN1-3*), and one member of a set of B-type cyclin genes (*CLB1-6*) (*1–4*). A key insight into the molecular switch that drives cells from G_1 to the S phase was the observation that the G_1/S cell cycle arrest of *cdc34*^{ts}, *cdc4*^{ts}, *cdc53*^{ts}, and *skp1*^{ts} mutants is suppressed by deletion of *SIC1*, which encodes an inhibitor of the protein kinase activity of a set of S phase–promoting Clb/Cdc28p complexes (*1*, *3*). Biochemical reconstitution experiments have revealed that Cdc4p, Cdc53p, and Skp1p constitute a ubiquitin ligase complex (SCF^{Cdc4}) that collaborates with the ubiquitin-conjugating enzyme Cdc34p and the G_1-specific Cdk Cln2p/Cdc28p (G_1 Cdkl) to promote the ubiquitination of Sic1p (*5*, *6*). Taken together, these data suggest that the destruction of Sic1p via the SCF^{Cdc4} ubiquitination pathway might trigger S phase entry in wild-type budding yeast cells.

G_1 Cdk activity is thought to be required for entry into S phase in all eukaryotic cells, but its exact targets have remained elusive. Sic1p is a potential key substrate of the budding yeast G_1 Cdk, because Cln proteins are required for Sic1p degradation in vivo and ubiquitination in vitro (*2*, *5*), and Cln function is dispensible in cells lacking Sic1p (*2*, *7*). Thus, Cln proteins might trigger Sic1p destruction and entry into S phase by modulating the activity of the Sic1p degradation machinery or by phosphorylating Sic1p directly, thereby allowing it to be recognized as a substrate for proteolysis.

There are nine (Ser or Thr) Pro candidate G_1 Cdk phosphoacceptor sites in Sic1p, seven of which (Fig. 1A) are clustered in the first 105 NH_2-terminal residues. This segment of Sic1p contains sequences that are both necessary and sufficient to specify Cdc34p-dependent ubiquitination (*5*). To test whether Sic1p serves as a substrate for G_1 Cdk, we mixed a purified maltose-binding protein–Sic1p chimera (MBP-Sic1p^{mycHis6}; myc and His6 refer to a bipartite epitope tag appended to the COOH-terminus of the hybrid protein) (*8*) with Cln2p/Cdc28p^{HA}/Cks1p complexes that were immunoaffinity-purified from insect cell lysates by virtue of the hemagglutinin (HA) tag appended to Cdc28p (*9*). MBP-Sic1p^{mycHis6} was efficiently phosphorylated by eluted G_1 Cdk complexes (Fig. 1B) but not by control eluates prepared from Sf9 cells expressing only Cln2p or Cdc28p. Unfused MBP was not phosphorylated by G_1 Cdk complexes despite its having two potential Cdk phosphorylation sites.

To map the sites at which MBP-Sic1p^{mycHis6} was phosphorylated by G_1 Cdk complexes, we used a multidimensional electrospray mass spectrometry (ESMS) technique (*10–12*). Tryptic phosphopeptides derived from purified phosphorylated MBP-Sic1p^{mycHis6} (Fig. 1C) were isolated by high-performance liquid chromatography (HPLC) followed by ESMS in the negative ion mode through single-ion monitoring of PO_3^-, which has a mass-to-charge ratio (m/z) of 79. The m/z 79 ion is a specific marker for phosphopeptides; the distribution of this ion (Fig. 1D, gray) is superimposed on the 214-nm

R. Verma, G. Reynard, R. J. Deshaies, Division of Biology, Box 156-29, California Institute of Technology, Pasadena, CA 91125, USA. E-mail for R.J.D.: deshaies@cco.caltech.edu

R. S. Annan, M. J. Huddleston, S. A. Carr, Research Mass Spectrometry Laboratory, SmithKline Beecham Pharmaceuticals, King of Prussia, PA 19406, USA.

Table 1. Summary of ESMS analysis of phosphopeptides from in vivo– and in vitro–phosphorylated Sic1p (*17*).

Sites	HPLC fraction	Molecular size measured/ calculated	Peptide*	Number of PO_3 groups (mol%)†
			In vitro	
T5	19–20	1909.8/?‡	(?) . . . EFMAPS**T**PPR (8)	1
T22–S25	16–17	2048.8/2048.3§	(14) YLAQPSGN**TSSS**ALMQGQK (32)	1–2‖
T33, 45, 48	16–17	2163.2/2163.5¶	(33) **T**PQKPSQNLVPV**T**PS**T**TK (50)	3#
S69, 76, 80	24	3509.5/3510.1	(54) NAPLLAPPNSNMGMTSPFNGL TSPQRSPFPK (84)	3–4
T173	16–17	1349.6/1349.6	(166) IIKDVPG**T**PSDK (177)	1
S191	12–13	1053.2/1053.4	(186) NWNNN**S**PK (193)	1
			In vivo	
T5	24, 25	1048.0/1047.6§	(2) APS**T**PPR (8)**	0 (ND) 1 (100%)
T33††	53–55	4032.0/4031.1§	(14) YLAQPSGNTSSSALMQGQK**T**PQK KPSQNLVPVTPST TK (50)	0 (58%) 1 (28%) 2 (14%)
S76‡‡	69–73	3348.0/3347.6§	(54) NAPLLAPPNSNMGMTSPFNGL [**TS**]PQRSPFPK (84)	0 (67.7%) 1 (23%) 2 (4.5%) 3 (4.8%)

*Numbers in parentheses refer to the first and last amino acid of each peptide. Amino acids indicated in large boldface type were deduced to be phosphorylated on the basis of ESMS-based sequencing. †Number of PO_3 groups detected per peptide; mol% indicates the fraction of a given peptide that was detected in a particular phosphorylation state with positive-ion ESMS. N.D.: not detected. ‡Calculated mass is unknown because we do not know the exact amino acid sequence across the MBP-Sic1p junction. Nevertheless, phosphorylation of T5 was directly confirmed by sequencing residues from the COOH-terminus of the peptide. §Masses given are those of the singly phosphorylated peptide. ‖Two phosphate residues are distributed over T21-S25, with no single site phosphorylated at high stoichiometry. ¶Masses given are those of the triply phosphorylated peptide. #T21-S25, T33, T45, and T48 were also recovered on peptide 14–50, which was detected in triply (10.5%), quadruply (26.3%), and quintuply (63.2%) phosphorylated states. **The initiator methionine was not present. ††T33 was also recovered on peptides 11–50, 11–53, and 14–53. In each case, the peptides were recovered with 0, 1, and 2 mol of PO_3 in ratios similar to those reported for the 14–50 peptide. ‡‡ESMS-based sequencing was unable to distinguish whether phosphate resided on T75 or S76.

ultraviolet (UV) chromatogram (Fig. 1D). HPLC fractions shown to contain phosphopeptides were reanalyzed by nanoelectrospray (nanoES) MS (*13*), with a precursor ion scan of m/z 79 to define the molecular weights of the phosphopeptides. Locations of modified residues within phosphopeptides were then determined by sequencing that used collision-induced dissociation tandem MS. All eight potential Cdk phosphorylation sites within MBP-Sic1p^{mycHis6} [the ninth site at Thr^2 was changed to Ala during cloning into the expression vectors (*8*)] appeared to be quantitatively phosphorylated in vitro (Table 1). The presence of phosphate was directly confirmed by tandem MS–based sequencing for residues 5, 33, 45, 173, and 191 and was inferred (by mass and partial sequence data) for residues 69, 76, and 80. Two-dimensional thin-layer chromatography of tryptic peptides derived from in vitro–phosphorylated wild-type and Ser^{76} → Ala^{76} (S76A) mutant Sic1p^{HA} confirmed that Ser^{76} was phosphorylated (*14*). Modification was also observed at the nonconsensus sites Thr^{22} and Ser^{23} through Ser^{25}, which were phosphorylated poorly, and Thr^{48}, which was phosphorylated quantitatively (Table 1). The long incubation of kinase with substrate may have compromised the specificity of the kinase reaction. However, no phosphopeptides were recovered from the MBP domain of the hybrid protein.

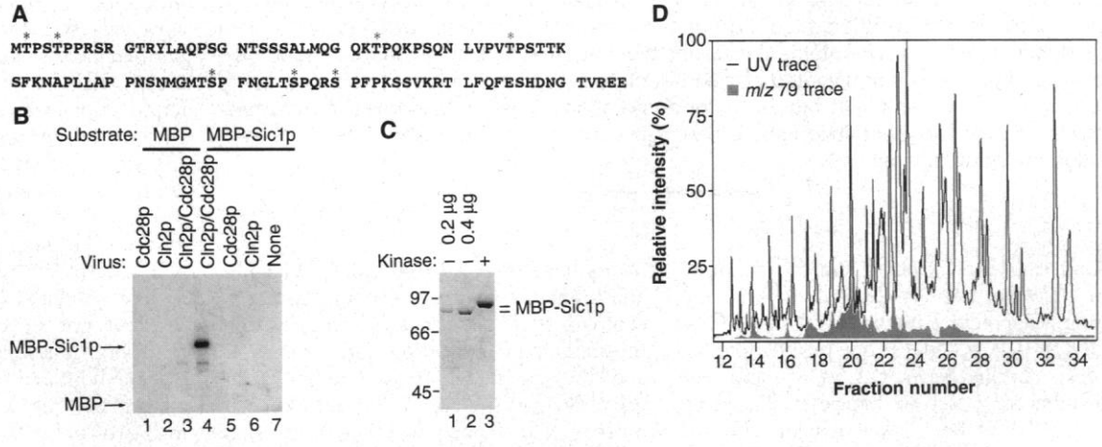

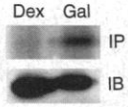

Fig. 1. G_1 Cdk–dependent phosphorylation of Sic1p in vitro and in vivo. (**A**) Amino acid sequence of the NH_2-terminal 105 residues of Sic1p (*17*). Potential Cdk phosphoacceptor sites are marked with an asterisk. This fragment is sufficient to serve as a substrate for Cln2p- and Cdc34p-dependent ubiquitination (*5*). The complementary COOH-terminal domain, which is dispensible for ubiquitination, has two additional consensus sites at Thr^{173} and Ser^{191}. (**B**) Phosphorylation of MBP-Sic1p^{mycHis6} by G_1 Cdk complexes. Sf9 insect cells were either singly or doubly infected with recombinant baculoviruses encoding Cdc28p^{HA} or Cln2p, as indicated. Lysates prepared from infected (lanes 1 through 6) or uninfected (lane 7) Sf9 cells were activated by addition of Cks1p and adsorbed to 12CA5 beads (protein A–Sepharose beads cross-linked to an α-HA monoclonal antibody). The activated kinase complex was eluted with the HA peptide (*28*) and assayed for MBP-Sic1p^{mycHis6} protein kinase activity (*25*). MBP-Sic1p^{mycHis6} was purified from *E. coli* (*29*). (**C**) Coomassie blue–stained SDS-polyacrylamide gel of 0.2 and 0.4 μg of unmodified MBP-Sic1p^{mycHis6} (lanes 1 and 2) and phosphorylated MBP-Sic1p^{mycHis6} (lane 3) used for phosphopeptide mapping. MBP-Sic1p^{mycHis6} was phosphorylated with G_1 Cdk complexes as described (*28*). (**D**) HPLC profile of typsin-digested phospho–MBP-Sic1p^{mycHis6}. Trypsin digests were loaded on a reversed-phase column; and after the UV detector, the column eluent was split, with 90% collected as fractions and 10% sent directly to the mass spectrometer, which was operated in the negative-ion mode and optimized to detect m/z 79 product ions (PO_3^-) generated by collision-induced dissociation before the first quadrupole (*27*). Material absorbing at 214 nm (clear trace) was overlain with the m/z 79 product ion trace (gray trace) to identify phosphopeptide-containing fractions. (**E**) Sic1p is phosphorylated in vivo by a Cln-dependent kinase. An exponential culture of *cdc34-2 cln1,2,3-Δ GAL-CLN3* (RJD768) cells at 24°C was transferred from phosphate-free YP-galactose (gal) medium to dextrose (dex) medium to effect Cln depletion and G_1 arrest. Arrested cells were shifted to 37°C for 1 hour, after which the culture was split into two halves, which were harvested and resuspended in galactose or dextrose medium. After a further 1-hour incubation at 37°C, cells were labeled with carrier-free phosphate (1 mCi per 25 OD units). Cell extracts were prepared and immunoprecipitated with antiserum to Sic1p as described (*30*), and immunoprecipitates were evaluated by autoradiography (IP, top panel) and immunoblotting with antiserum to Sic1p (IB, bottom panel).

Mutant *cdc34*^{ts} cells arrest with high Cln/Cdc28p protein kinase activity (*15*) and accumulate phosphorylated Sic1p (*1*, *2*). To test directly if phosphorylation of Sic1p in vivo was dependent on Cln/Cdc28p kinase activity, *cdc34*^{ts} *cln1,2,3-Δ GAL-CLN3* cells were first arrested in G_1 at 24°C by extinguishing *CLN3* expression in dextrose medium, and then shifted to 37°C to inactivate Cdc34p. After 1 hour of incubation, the culture was split in two: one half was resuspended in galactose medium (*CLN3* expression on) and the other in dextrose medium (*CLN3* expression off). After a further incubation at 37°C for 1 hour, cells were labeled with ^{32}P. As shown in Fig. 1E, Sic1p isolated from cells expressing *CLN3* contained at least 12 times more phosphate (as determined by PhosphorImager analysis) than did Sic1p isolated from cells depleted of *CLN3*. Thus, Sic1p phosphorylation in vivo was largely dependent on G_1 Cdk activity.

To identify the sites at which Sic1p was phosphorylated in vivo, we purified Sic1p^{HAHis6} from *cdc34*^{ts} cells, digested it with trypsin, and analyzed the resulting peptides by multidimensional ESMS (*16*). Precursor ion scanning and sequencing by nanoES tandem MS of phosphopeptide-containing fractions (Table 1) revealed the following. (i) Peptide 2–10 (numbers refer to the amino acids that the peptide spans) was phosphorylated quantitatively on Thr^5. (ii) Several distinct phosphopeptides encompassing residues Thr^{33} and Thr^{45} each contained 1 to 2 mol of phosphate, and direct MS-based sequencing of singly phosphorylated 14–53 peptide (doubly phosphorylated peptide could not be recovered for sequencing) excluded all S and T residues as being phosphorylated, except for Thr^{33}. (iii) A peptide containing Ser^{76} (54–84) was identified in singly, doubly, and triply phosphorylated forms, and direct MS-based sequencing of the singly phosphorylated peptide (once again, multiply phosphorylated peptides could not be recovered for sequencing) excluded all Ser and Thr residues as being phosphorylated, except for Thr^{75} and Ser^{76}. Given the in vitro mapping data above and the mutagenesis results described below, we conclude that Ser^{76} was phosphorylated in vivo.

The detection of six phosphates among the tryptic phosphopeptides (Table 1) agrees well with the predicted phosphorylation state of the intact starting material, as determined by positive ion ESMS: >88% of the Sic1p^{HAHis6} purified from *cdc34*^{ts} cells had one to six phosphates per molecule (*14*). Although we obtained no direct evidence for in vivo phosphorylation of Thr^{22}, Ser^{23} to Ser^{25}, Thr^{45}, Thr^{48}, Ser^{69}, and Ser^{80}, a subset of these sites may have been modified on the doubly and triply phosphorylated 14–50 and 54–84 peptides that we failed to recover for sequencing. Moreover, to obtain sufficient quantities of Sic1p^{HAHis6} for analysis, the protein was transiently overexpressed from the *GAL* promoter. This overproduction may have taxed the ability of G_1 Cdk complexes to maintain Sic1p^{HAHis6} in a maximally phosphorylated state.

To test their role in Sic1p destruction, we mutagenized phosphoacceptor sites of Sic1p detected by ESMS either singly or in various combinations. The mutants were then tested for their ability to serve as ubiquitination substrates with the use of a Cln2p- and Cdc34p-dependent in vitro ubiquitination assay (*5*). The effects of mutations in Thr^{173} and Ser^{191} were not examined, because an NH_2-terminal 160–amino acid segment of Sic1p is both necessary and sufficient to direct its Cdc34p- and Cln2p-dependent ubiquitination (*5*). Whereas the single point mutants in which Thr^2 (*14*), Ser^{69}, and Ser^{80} were changed to Ala were as efficiently ubiquitinated as was wild-type Sic1p^{HAHis6}, T2A/T5G, T33A, and S76A mutants (*17*) exhibited a modest decrease in ubiquitination, and the T45A mutant was poorly ubiquitinated (Fig. 2A). Because none of the point mutations eliminated Sic1p^{HAHis6} ubiquitination, we analyzed the effect of the T2A/T5G, T33A, T45A, and S76A mutations in various combinations. Double mutants (T2A/T5G was considered as a single mutant) invariably were poorer ubiquitination substrates than single mutants. All triple mutants analyzed, including one lacking three in vivo phosphoacceptor sites identified by ESMS (Sic1p-Δ3P: T5G, T33A, and S76A), had a severe ubiquitination defect (Fig. 2, A and B). Mutating these residues did not result in global misfolding of Sic1p-Δ3P, as assayed by its ability to bind Clb5p^{HA} (Fig. 2B) and inhibit Clb5p-associated kinase activity (*14*). Although the Sic1p-Δ3P mutant was impaired in its ability to serve as a ubiquitination substrate, it was still phosphorylated in vitro and in vivo, although to a lesser extent than wild-type Sic1p (*14*). In sum, the mutational analysis suggested that Sic1p must be phosphorylated on a subset of sites by G_1 Cdk complexes to serve as a substrate for the Cdc34p pathway, but that phosphorylation of no single site within this subset was either sufficient or absolutely necessary to target Sic1p for Cdc34p-dependent ubiquitination.

The G_1/S arrest phenotype of *skp1*^{ts}, *cdc4*^{ts}, *cdc53*^{ts}, and *cdc34*^{ts} mutants can be suppressed by deleting *SIC1*, which suggests

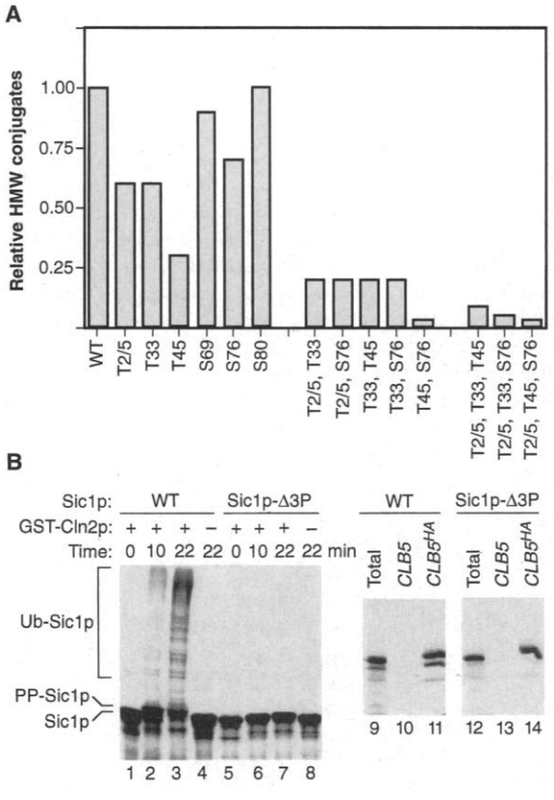

Fig 2. In vitro ubiquitination of Sic1p mutants lacking sites of phosphorylation. (**A**) Single and combinatorial point mutants of Sic1p^{HA} were generated by PCR and transcribed and translated in wheat germ extract supplemented with [^{35}S]methionine (*31*). Wild-type and mutant Sic1p^{HA} translation products were assayed for ubiquitination as described (*5*, *26*). In vitro ubiquitination reactions were resolved on 10% SDS-polyacrylamide gels and quantitated with a PhosphorImager (Molecular Dynamics) (*32*). (**B**) Sic1p-Δ3P (Sic1p^{HA} carrying the T2A/T5G, T33A, and S76A substitutions) was poorly ubiquitinated but nonetheless bound tightly to Clb5p/Cdc28p. (Left panel) Wild-type and mutant Sic1p^{HA} were assayed for ubiquitination as described in (A). Incubations proceeded for 0, 10, or 22 min in the presence or absence of glutathione S-transferase (GST)–Cln2p (*5*) as indicated. Ub-Sic1p, PP-Sic1p, and Sic1p refer to ubiquitinated, phosphorylated, and unmodified Sic1p^{HA}, respectively. Wild-type and mutant Sic1p^{HA} translation products were mixed with extracts prepared from either *CLB5* or *CLB5*^{HA} cells, as indicated (right panel). One-third of the total input protein is depicted in lanes 9 and 12, and 12CA5 precipitates are depicted in lanes 10, 11, 13, and 14. Cell extracts and immunoprecipitates with 12CA5 were prepared as described (*5*).

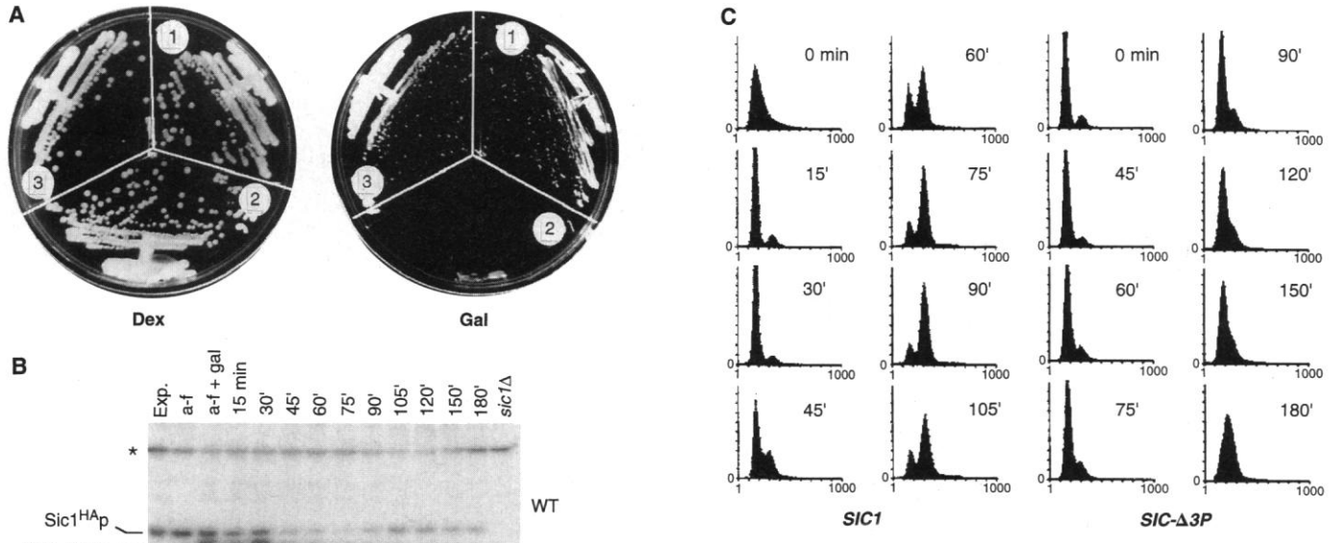

Fig. 3. Sic1p-Δ3P is stable in vivo and blocks DNA replication. (**A**) Constitutive expression of *SIC1Δ3P* is toxic. RJD1025 (sector 1; W303 plus *sic1::SIC1HAHis6::TRP1, ura3::GAL-SIC1::URA3*), RJD1026 (sector 2; W303 plus *sic1::SIC1HAHis6::TRP1, ura3::GAL-SIC1-Δ3P::URA3*), and RJD730 (sector 3; W303 plus *sic1::SIC1HAHis6::TRP1, ura3::GAL::URA3*) cells were streaked onto YP dextrose (dex; left) or YP galactose (gal; right) plates and incubated at 30°C for 3 days. (**B**) RJD1025 and RJD1026 cells grown in YP raffinose medium were arrested with a-factor (50 ng/ml) for 2.5 hours, and *SIC1* expression was induced transiently for 45 min by the addition of galactose to 2%. Cells were then transferred to fresh YP medium containing 2% dextrose, and portions were withdrawn every 15 min and processed for immunoblotting with antiserum to Sic1p, followed by secondary detection with [^{125}I-labeled donkey antibodies to a rabbit immunoglobulin F(ab')2 fragment. Antiserum to Sic1p detected both untagged Sic1p expressed from the *GAL* promoter andSic1p^{HAHis6} expressed from the natural *SIC1* promoter. Exp, a-f, and *sic1Δ* refer to exponentially growing cells, α-factor–arrested cells, and RJD1021 *sic1Δ* mutants, respectively. (**C**) The same cells used in (B) were stained with propidium iodide and analyzed by flow cytometry to evaluate cellular DNA contents (*33*).

that these mutants are unable to replicate because of accumulation of Sic1p, which in turn inhibits the S phase–promoting Clb5p/Cdc28p protein kinase (*1*, *3*). This interpretation is clouded by the fact that multiple proteins [including the G_1 Cdk inhibitor Far1p (*18*)] accumulate in these mutants. Furthermore, the cell cycle defect of Cdc34p pathway mutants might be ameliorated by eliminating a major target such as Sic1p because the temperature-sensitive growth phenotype of these mutants is sensitive to the dosage of substrates (*3*, *18*, *19*).

Thus, we tested whether Sic1p-Δ3P was stable in vivo and whether expression of nondegradable Sic1p-Δ3P would block DNA replication in wild-type cells. Regulated expression of Sic1p-Δ3P from the *GAL* promoter strongly inhibited cell proliferation in the presence of galactose (Fig. 3A). To evaluate the stability of Sic1p-Δ3P in vivo and the consequences of Sic1p-Δ3P expression on cell cycle progression, we arrested *GAL-SIC1-Δ3P* and *GAL-SIC1* strains in G_1 phase with α-factor, transiently activated expression of the *GAL* promoter for 45 min, and released the induced cells into dextrose medium lacking α-factor (Fig. 3B). *SIC1* transcripts expressed from the *GAL* promoter declined rapidly upon transfer to dextrose medium (*14*) . Immunoblotting with antiserum to Sic1p revealed that transient activation of the *GAL* promoter directed the accumulation of both Sic1p and Sic1p-Δ3P to amounts 1.5 times times that expressed from the *SIC1*^{HAHis6} allele residing at the natural *SIC1* locus (Fig. 3B). After release from cell cycle arrest, the amounts of Sic1p expressed from the *GAL* promoter and that of endogenous Sic1p^{HAHis6} declined in parallel at ~45 min, concomitant with the initiation of S phase as judged by flow cytometry (Fig. 3C). In contrast, Sic1p-Δ3P persisted for at least 3 hours (Fig. 3B), and most of the cells containing the *GAL-SIC1-Δ3P* allele failed to replicate their DNA during this time (Fig. 3C). In addition, Clb5p/Cdc28p kinase inhibitory activity (*1*) persisted indefinitely in cells expressing Sic1p-Δ3P but disappeared at ~45 min in cells expressing Sic1p (*14*).

A distinctive phenotype of Cdc34p pathway mutants is the gradual appearance of multiply budded cells in arrested cultures. Pheromone-synchronized cells that tran-

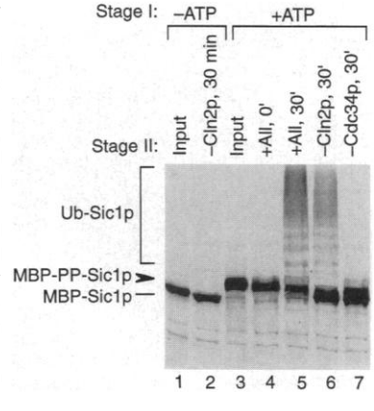

Fig. 4. Phosphorylation of Sic1p is sufficient to trigger Cdc34p-dependent ubiquitination. [^{35}S]labeled MBP-Sic1p^{mycHis6} was isolated from *E. coli* (*29*) and incubated in the absence (lanes 1 and 2) or presence (lanes 3 through 7) of 1 mM ATP with G_1 Cdk purified from baculovirus-infected Sf9 cells (stage I). After incubation, MBP-Sic1p^{mycHis6} was isolated on amylose resin and used as a ubiquitination substrate in stage II. Purified MBP-Sic1p^{mycHis6} was incubated with no further additions (lanes 1 and 3) or with Cdc34p- and Cln-depleted G_1 yeast extract (lanes 2 and 4 through 7) supplemented with Cdc34p (lanes 2 and 6) or GST-Cln2p (lane 7) or both (lanes 4 and 5). Ub, ubiquitinated; PP, phosphorylated. All reactions were incubated at 25°C for 30 min except that shown in lane 4 (0 min). Ubiquitination-competent yeast extracts were prepared and ubiquitination reactions were assembled as described (*5*).

siently expressed Sic1p-Δ3P likewise exhibited a multiply budded phenotype: Three hours after release from α-factor arrest, 69% of Sic1p-Δ3P–expressing cells were singly budded and 26% were multiply budded. Although Sic1p-Δ3P expression mimics the major characteristics of Cdc34p/SCF^{Cdc4} pathway mutants, it does not appear to inhibit the Cdc34p/SCF^{Cdc4} pathway, because the bulk of wild-type Sic1p^{HAHis6} was degraded on schedule in Sic1p-Δ3P–expressing cells (Fig. 3B).

To address whether phosphorylation of Sic1p by G_1 Cdk might be the primary cell cycle–regulated event that activates its destruction late in G_1 phase, we performed a two-step in vitro ubiquitination reaction. Purified ^{35}S-labeled MBP-Sic1p^{mycHis6} was incubated with or without adenosine triphosphate (ATP) with G_1 Cdk complexes immunoaffinity-purified from Sf9 cells. MBP-Sic1p^{mycHis6} was then re-isolated and added to yeast extract prepared from Cln-depleted cells. MBP-Sic1p^{mycHis6} derived from kinase incubations lacking ATP was neither phosphorylated nor ubiquitinated in yeast extract lacking Cln2p (Fig. 4), which confirms that the repurified MBP-Sic1p^{mycHis6} was not contaminated with G_1 Cdk complex. In contrast, phospho–MBP-Sic1p^{mycHis6} was ubiquitinated by yeast extract in a Cdc34p-dependent manner regardless of whether Cln2p was present. Ubiquitination of phospho–MBP-Sic1p^{mycHis6} was modestly enhanced, however, by the inclusion of Cln2p in the second step. Thus, whereas G_1 Cdk might modestly augment the activity of Cdc34p or SCF^{Cdc4}, it is not absolutely required for the activity of this ubiquitination pathway.

We envision the following sequence of events for the G_1/S transition in budding yeast. In early G_1 cells, stable Sic1p quenches the activity of S phase–promoting Clb/Cdc28p complexes. In late G_1 cells, G_1 Cdk, which is insensitive to the inhibitory action of Sic1p, is activated and phosphorylates Sic1p on multiple residues. Such multisite phosphorylation may impart cooperativity to the G_1/S transition (*20*). Whereas unmodified Sic1p is stable despite the presence of an active Cdc34p/SCF^{Cdc4} pathway in G_1 cells, phospho-Sic1p is efficiently recognized by SCF^{Cdc4} (*6*), ubiquitinated, and degraded by the 26S proteasome. Thus, G_1 Cdk–dependent phosphorylation of Sic1p is the key regulated event that sets in motion the transition from G_1 phase to S phase. An important question is, is S phase entry governed by a similar process in other eukaryotes? Whereas the Cdc4p homolog Pop1 is not required for DNA replication in fission yeast (*21*), progression into S phase in animal cells is restrained by the Cdc34p substrate p27Kip1 (*22*), and inhibition of Cdc34p activity blocks S phase in *Xenopus* extracts (*23*). Substrate phosphorylation has been implicated in the regulated destruction of multiple metazoan proteins, including key signaling proteins such as IκB and B-catenin (*24*). The extensive use of substrate phosphorylation to regulate protein stability may foreshadow a broadly conserved mechanism for regulated protein destruction in eukaryotic cells (*6*).

REFERENCES AND NOTES

1. E. Schwob, T. Böhm, M. Mendenhall, K. Nasmyth, *Cell* **79**, 233 (1994).
2. B. L. Schneider, Q. H. Yang, A. B. Futcher, *Science* **272**, 560 (1996).
3. C. Bai *et al.*, *Cell* **86**, 263 (1996).
4. N. Mathias *et al.*, *Mol. Cell. Biol.* **16**, 6634 (1996).
5. R. Verma, R. M. R. Feldman, R. J. Deshaies, *Mol. Biol. Cell* **8**, 1427 (1997b).
6. R. M. R. Feldman, C. C. Correll, K. B. Kaplan, R. J. Deshaies, *Cell*, in press; D. Skowyra *et al.*, *ibid.*, in press.
7. M. Tyers, *Proc. Natl. Acad. Sci. U.S.A.* **93**, 7772 (1996); L. Dirick, T. Böhm, K. Nasmyth, *EMBO J.* **14**, 4803 (1995).
8. Detailed descriptions of all plasmid constructs used in this study are available upon request. In all of the *SIC1* plasmid constructs described in this report, the Thr at position 2 was converted to an Ala as part of the cloning strategy used to insert *SIC1* in expression vectors. Unlike the T2A T5G double mutation (Fig. 2A), the T2A conversion had no effect on the ability of Sic1p to serve as a substrate for ubiquitination (*14*) . In the *SIC1-Δ3P* mutant expressed in vivo, Thr^5 was mutated to Gly Pro. Sic1p^{HAHis6} and Sic1p^{mycHis6} contained the sequences RPYPYDVPDYASLGYHHHHHHGP and RPLEEQKLISEEDLLRHHHHHHGP (*17*), respectively, inserted immediately upstream of the COOH-terminal histidine. Sic1p^{HA} contained the sequence QSRDQEHPYPYDVPDYASLG (*17*). These epitope tags had no effect on the ability of Sic1p to bind Clb5p or to serve as a substrate for ubiquitination in vitro.
9. Cln2p and Cdc28p^{HA} failed to form an active protein kinase complex upon expression from baculovirus vectors in Sf9 cells. Addition of the Cdk-binding Cks1p protein to Sf9 cell lysates, however, was sufficient to activate Cln2p/Cdc28p^{HA} complexes (*25*). In all experiments described in this report, G_1 Cdk refers to the baculovirus-expressed Cln2p/Cdc28p^{HA} complex that was activated by *Escherichia coli*–expressed Cks1p.
10. R. S. Annan and S. A. Carr, *J. Protein C* **16**, 391 (1997).
11. S. A. Carr, M. J. Huddleston, R. S. Annan, *Anal. Biochem.* **239**, 180 (1996).
12. M. J. Huddleston, R. S. Annan, M. F. Bean, S. A. Carr, *J. Am. Soc. Mass. Spectrom.* **4**, 710 (1993).
13. M. Wilm and M. Mann, *Anal. Chem.* **68**, 1 (1996).
14. R. Verma *et al*, data not shown.
15. M. Tyers, G. Tokiwa, B. Futcher, *EMBO J.* **12**, 1955 (1993).
16. RJD 1044 (*GAL-SIC1^{HAHis6}*, *cdc34-2*) cells were grown in 6 liters of 19% yeast extract and 2% peptone (YP) plus raffinose at 24°C to an optical density (OD_{600}) of 0.5. Sic1p^{HAHis6} synthesis was induced by the addition of galactose to 2%, and after 3 hours the culture was shifted to 37°C for a further 3 hours. Cells were ground in liquid nitrogen (*26*) . Five volumes of denaturing lysis buffer [DLB: 100 mM sodium phosphate, 10 mM tris, and 6 M guanidine hydrochloride (pH 8.0)] was added to 40 g of frozen cell powder, and the slurry was rotated end over end for 30 min at 24°C and then centrifuged at 26,000*g* for 15 min. The supernatant was mixed with 2 ml of nickel–nitrilotriacetic acid (Ni-NTA) resin for 40 min at 24°C, after which the beads were washed twice with 20 ml DLB; twice with 100 mM sodium phosphate (pH 5.9), 10 mM imidazole, and 2 M urea; and twice with 25 mM tris (pH 8.0), 500 mM NaCl, and 0.2% Triton X-100. Bound proteins were eluted with 250 mM imidazole, 50 mM tris (pH 8.0), and 250 mM NaCl; and the eluate was supplemented with NaCl (500 mM), Triton X-100 (0.2%), a protease inhibitor cocktail (5 mM EDTA, 2 mM EGTA, 0.2 mM 4-(2-aminoethyl)-benzene sulfonyl fluoride hydrochloride, leupeptin (5 μg/ml) and pepstatin, and 0.5 mM phenylmethylsulfonyl fluoride), and a phosphatase inhibitor cocktail (10 mM NaF, 60 mM β-glycerophosphate, and 10 mM sodium pyrophosphate) to the indicated concentrations. The Ni-NTA eluate was then incubated for 45 min at 4°C with 12CA5 beads, after which the beads were collected by centrifugation and washed twice with binding buffer and three times with 10 mM tris (pH 6.8). Sic1p^{HAHis6} was eluted with 0.1% trifluoroacetic acid and processed for ESMS as described for in vitro–phosphorylated MBP-Sic1p^{mycHis6} (*27*).
17. Single-letter abbreviations for the amino acid residues are as follows: A, Ala; C, Cys; D, Asp; E, Glu; F, Phe; G, Gly; H, His; I, Ile; K, Lys; L, Leu; M, Met; N, Asn; P, Pro; Q, Gln; R, Arg; S, Ser; T, Thr; V, Val; W, Trp; and Y, Tyr.
18. S. Henchoz *et al.*, *Genes Dev.*, in press.
19. R. J. Deshaies, V. Chau, M. Kirschner, *EMBO J.* **14**, 303 (1995); A. R. Willems *et al.*, *Cell* **86**, 453 (1996).
20. J. E. Ferrell, *Trends Biochem. Sci.* **21**, 460 (1996).
21. K.-I. Kominami and T. Toda, *Genes Dev.* **11**, 1548 (1997).
22. S. Coats, W. M. Flanagan, J. Nourse, J. M. Roberts, *Science* **272**, 877 (1996); M. Pagano *et al.*, *ibid.* **269**, 682 (1995).
23. P. R. Yew and M. W. Kirschner, *ibid.* **277**, 1672 (1997).
24. H. Aberle, A. Baueer, J. Stappert, A. Kispert, R. Kemler, *EMBO J.* **16**, 3797 (1997); I. M. Verma *et al.*, *Genes Dev.* **9**, 2723 (1995).
25. G. J. Reynard and R. J. Deshaies, in preparation.
26. R. Verma, Y. Chi, R. J. Deshaies, *Methods Enzymol.* **283**, 366 (1997a).
27. Sic1p phosphorylated in vitro (350 pmol) or purified from cells (500 pmol) was digested with modified trypsin (Promega) for 16 hours at 37°C at an enzyme:substrate ratio of 1:7 (w/w). The tryptic digest was then subjected to a multidimensional phosphopeptide analysis with ESMS (*10*). In the first dimension, tryptic peptides were separated by microbore HPLC on a Reliasil C18 column (1 mm inside diameter) and analyzed with negative-ion ESMS on a PE-Sciex API electrospray triple quadrupole mass spectrometer. Approximately 10% of the HPLC eluent was directed to the mass spectrometer, and the remaining 90% was collected as fractions. The mass spectrometer was optimized to produce and detect collisionally induced product ions of *m/z* 79 (PO_3^-), which are diagnostic for phosphorylated peptides (*12*). The spectrometer was operated in a single-ion monitoring mode for enhanced sensitivity. The detection of the *m/z* 79 ion identified fractions that contained phosphopeptides, which were subsequently analyzed in the second dimension by negative-ion nanoelectrospray with selective detection for phosphopeptide precursors or parent ions [$(M-H)^-$; $(M-2H)^{2-}$; $(M-3H)^{3-}$; and so on] (*13*). When possible, a third dimension of analysis was carried out in the positive-ion mode, in which the complete product-ion mass spectrum was collected, thereby yielding sequence data from the phosphopeptide.
28. Lysates prepared from Sf9 cells coinfected with baculovirus constructs encoding Cln2p and Cdc28p^{HA} were activated by incubation with Cks1p (*25*) and purified as follows. A portion (400 μl) of insect cell lysate (~4 mg/ml) was mixed with 12CA5 beads (100 μl packed volume) and incubated for 4 hours at 4°C. The resin was then washed twice with IPB buffer [50 mM β-glycerophosphate (pH 7.5), 100 mM NaCl, 5 mM EDTA, and 0.2% Triton-X100] and twice with elution buffer [20 mM Hepes (pH 7.4), 100 mM NaCl, and 2 mM dithiothreitol (DTT)]. Bound kinase complexes were eluted overnight at 4°C in 100 μl of elution buffer containing HA peptide [YPYDVPDYASL (*17*); 1 μg/ml]. Eluted kinase (350 μl) and substrate (MBP-Sic1p^{mycHis6}; 100 μg) were mixed together and adjusted to 50 mM tris (pH 7.5), 10 mM $MgCl_2$, 2 mM DTT, and 2 mM ATP (750 μl final volume). After a 4-hour incubation at 24°C, a protease and phosphatase inhibitor cocktail was

added (16), and phospho–MBP-Sic1p^{mycHis6} was purified away from the reaction components by adsorption to 9E10 beads (monoclonal antibody to myc covalently coupled to protein A–Sepharose). Beads were washed twice with 25 mM tris (pH 8.0), 500 mM NaCl, and 0.2% octylglucoside, then twice with 25 mM tris (pH 6.8). Phospho–MBP-Sic1p^{mycHis6} was eluted with 0.1% TFA, and the eluted protein was lyophilized in a Speedvac and reconstituted in 50 mM tris (pH 8.8) and 2 M urea.

29. MBP-Sic1^{mycHis6} was isolated from BL21(DE3) cells containing pLysS by means of consecutive fractionations on Ni-NTA (Qiagen) and amylose (New England BioLabs) affinity resins according to the manufacturer's recommended procedures. In Fig. 4, [^{35}S]-labeled MBP-Sic1p^{mycHis6} was expressed and purified from Tran^{35}S-labeled *E. coli* cells as described (26).
30. ^{32}P-labeled cells were harvested, vortexed with glass beads (0.5 mm), and then boiled in 2× lysis buffer containing 100 mM tris (pH 7.5), 2% SDS, 200 mM NaCl, 30 mM DTT, and a protease and phosphatase inhibitor cocktail (16). Cell lysates were diluted to a final concentration of 0.2% SDS with an immunoprecipitation buffer containing 50 mM tris (pH 7.5), 500 mM NaCl, 1% Triton X-100, and the phosphatase and protease inhibitor cocktails described above. Diluted lysates were centifuged at 15,000*g* for 15 min and supplemented with antiserum to Sic1p and protein A beads. Beads were washed three times with immunoprecipitation buffer and twice with 50 mM tris (pH 7.5) and were resuspended in 2× SDS sample buffer.
31. All singly and multiply mutated forms of *SIC1* were generated by a polymerase chain reaction (PCR)–based strategy (26) . PCR was done with 5' oligos containing T7 promoter sequences, and with a 3' oligo incorporating an HA epitope tag. Details are available upon request. In vitro transcription and translation of wild-type and mutant PCR templates were done as described (26).
32. The percentage of high-molecular-weight (HMW) ubiquitin conjugates formed was calculated by dividing the signal corresponding to ubiquitinated Sic1p^{HA} formed during a 30-min incubation in vitro by the total amount of Sic1^{HA} translation product present at the start of the reaction. Wild-type Sic1p^{HA} (65% of which was converted to HMW ubiquitin conjugates) was arbitrarily assigned a relative value of 1.0.
33. C. B. Epstein and F. R. Cross, *Genes Dev.* **6**, 1695 (1992).
34. We thank M. V. Castillo for MBP-SIC1, L. Johnston for Sic1p antiserum, S. Diamond for performing flow cytometry, J. Archer, B. Dunphy, and W. Shou for critically reading the manuscript, and members of the laboratory for helpful discussions. Supported in part by Searle/Chicago Community Trust and Lucille P. Markey Charitable Trust Scholar Awards to R.J.D. and by a grant from NIH (NIH RO1 GM52466-01).

16 June 1997; accepted 18 September 1997

CDC20 and *CDH1*: A Family of Substrate-Specific Activators of APC-Dependent Proteolysis

Rosella Visintin, Susanne Prinz, Angelika Amon*

Proteolysis mediated by the anaphase-promoting complex (APC) triggers chromosome segregation and exit from mitosis, yet its regulation is poorly understood. The conserved Cdc20 and Cdh1 proteins were identified as limiting, substrate-specific activators of APC-dependent proteolysis. *CDC20* was required for the degradation of the APC substrate Pds1 but not for that of other APC substrates, such as Clb2 and Ase1. Conversely, *cdh1*Δ mutants were impaired in the degradation of Ase1 and Clb2 but not in that of Pds1. Overexpression of either *CDC20* or *CDH1* was sufficient to induce APC-dependent proteolysis of the appropriate target in stages of the cell cycle in which substrates are normally stable.

Progression through mitosis requires the precisely timed ubiquitin-dependent degradation of specific substrates. In budding yeast, degradation of the Pds1 protein is required for the transition from metaphase to anaphase in the cell cycle (1). Exit from mitosis is initiated by proteolysis of mitotic cyclins (2). Destruction of the mitotic spindle–associated protein Ase1 is important for the disassembly of the mitotic spindle during exit from mitosis (3). Degradation of all these proteins is mediated by a 20S particle called the cyclosome or APC, which functions as a ubiquitin-protein ligase (4, 5). The stability of substrates of the APC-dependent proteolysis machinery varies greatly during the cell cycle. Substrates are stable during S phase, G_2 phase, and early mitosis (M) phase but are highly unstable during exit from M phase and G_1 phase (1, 3, 6–8). Work in embryonic extracts has shown that APC activity is cell cycle regulated, suggesting that the activity of the APC determines whether APC substrates are degraded or not (4, 5). However, degradation of different APC substrates is not coordinated, because temporal differences are observed (9–11). The proteolysis of APC substrates, therefore, cannot simply be regulated by the activation or inactivation of APC. Regulation must also occur at the level of specific substrates. We identified two highly conserved *Saccharomyces cerevisiae* proteins that function in this manner. Cdc20 and Cdh1 are substrate-specific activators of APC-dependent proteolysis.

To identify regulators of APC-dependent proteolysis, we screened previously identified temperature-sensitive cell division cycle (*cdc*) mutants for defects in APC-dependent proteolysis. Among these, mutants defective in the *CDC20* gene, which encodes a protein containing seven WD40 repeats (12), were of particular interest. *Saccharomyces cerevisiae cdc20-1* mutants and *Drosophila* mutants defective in the *fizzy* gene, a *CDC20* homolog, arrest in metaphase before the activation of the APC-dependent proteolytic program (11–14). To analyze the effects of the *cdc20-1* mutation on APC-dependent proteolysis, we took advantage of the fact that in yeast all known APC substrates (the mitotic cyclins Clb2 and Clb3, Pds1, and Ase1) are unstable during G_1 phase because of continuous APC-dependent proteolysis (1, 3, 7, 15). Wild-type and *cdc20-1* cells were arrested at the permissive temperature in G_1 phase by exposure to the mating pheromone α-factor, and the half-lives of Clb2, Pds1, and Ase1 were determined after transient expression of their respective genes from the galactose (Gal)-inducible *GAL1-10* promoter and inactivation of *CDC20* by temperature shift (16). The *cdc20-1* mutation had little if any effect on the half-life of Clb2 (Fig. 1, A and B), which is consistent with the finding that the *cdc20-1* mutation does not affect ubiquitination of Clb2 in G_1 phase extracts (15). Similarly, the *cdc20-1* mutation had little if any effect on the half-life of Ase1 during G_1 phase (Fig. 1, C and D). In contrast, the half-life of Pds1 was prolonged in the *cdc20-1* mutant; Pds1 protein declined rapidly in wild-type cells but not in *cdc20-1* mutants (Fig. 1, E and F). These results indicate that *cdc20-1* mutants are defective in the degradation of Pds1 but not in that of Clb2 and Ase1 during the G_1 phase.

Because *CDC20* was required for the degradation of Pds1, we hypothesized that overexpression of *CDC20* might hasten the degradation of Pds1. To test this hypothesis, we treated exponentially growing cells carrying *CDC20* under the control of the *GAL1-10* promoter (17) with Gal to induce increased expression of *CDC20*. Although overexpression of *CDC20* did not affect the amount of *PDS1* RNA (18), the bulk of Pds1 protein disappeared within 60 min of Gal addition (Fig. 2A). In contrast, overexpression of *CDC20* had little if any effect on the total amounts of Clb2 or Ase1 protein (Fig. 2A). The decline in the amount of Pds1 brought about by overexpression of *CDC20* was prohibited in cells carrying a

Whitehead Institute for Biomedical Research, Nine Cambridge Center, Cambridge, MA 02142, USA.

*To whom correspondence should be addressed.